TAO, Vol. 9, No. 3, 395-408, September 1998

Preliminary Results of a Large Offset Seismic Survey West of Hengchun Peninsula, Southern Taiwan

Yosio Nakamura[1], Kirk McIntosh[1] and Allen T. Chen[2]

(Manuscript received 11 March 1998, in final form 22 July 1998)

ABSTRACT

As a part of the U.S.-R.O.C. collaborative deep seismic imaging experiment, six ocean-bottom seismographs (OBSs) were deployed along the 12°12'N parallel west of Hengchun Peninsula and wide-offset seismic signals from a large air-gun array shot over the line were recorded. A preliminary analysis of these data together with those from another OBS to the east of the peninsula reveals that a 11-km thick crustal layer, interpreted to be an extended continental crust of the southern margin of the Chinese mainland, lies under most of the line and dips toward the east at low angle. A complex margin wedge is observed at depth immediate west and underneath the peninsula, which may have resulted from the thick sedimentary layer, quite likely including the basement complex, pushed against the strong backstop provided by the Philippine Sea plate converging from the east.

(Key words: Southern Taiwan, Crustal structure, Subduction/Collision, Margin wedge, Ocean-bottom seismograph)

1. INTRODUCTION

The area in and around Taiwan is one of the tectonically most active areas on the surface of the earth. However, our understanding of the complex process of collision between two lithospheric plates, the Eurasian plate and the Philippine Sea plate, in the area is still incomplete despite extensive studies involving surface geology (e.g., Ho, 1986), geodesy (e.g., Yu, *et al.*, 1990), potential fields (e.g., Yeh, *et al.*, 1991), marine seismics (e.g., Lundberg, *et al.*, 1997), and natural seismicity (e.g., Wu, 1991). An important piece of information that was lacking from these previous studies is deep seismic structural data from the region. In order to fill this gap, a U.S.-R.O.C. collaborative deep seismic imaging experiment was conducted in the summer of 1995, wherein seismic signals along several seismic lines east and south of the island from a large air-gun array of *R/V Maurice Ewing* were recorded on a long hydrophone

[1]Institute for Geophysics, University of Texas at Austin, 4412 Spicewood Springs Road, Bldg. 600, Austin, TX 78759-8500, USA

[2]Institute of Applied Geophysics, National Taiwan Ocean University, Keelung, Taiwan, ROC

streamer, ocean-bottom seismographs (OBSs) and land stations.

The analysis of the vast quantity of acquire data has not yet been completed, pending combined interpretation of the entire data set from several diverse groups that participated in the experiment. This paper, therefore, is an attempt to present preliminary results from a set of OBS stations along a single seismic line, TAICRUST Line 33, lying west of Hengchun Peninsula at the southern tip of the island (Figure 1). We anticipate that publication of these results, together with similar papers in this volume covering other lines and line segments, will facilitate future interpretation of the combined data set.

2. TECTONIC BACKGROUND

Because of the oblique nature of the collision between the Eurasian plate and the Philippine Sea plate (Seno, 1977), the focus of intense deformation in and around Taiwan, caused mainly by the collision of the Luzon Arc on the Philippine Sea plate to the eastern continental margin of the Chinese mainland, has been progressing generally from north to south in the region (e.g. Huang, *et al.*, 1997). In this tectonic setting, the Hengchun Peninsula is located in the area of early collisional deformation, with highly deformed island of Taiwan to the north and pre-collision, simple subduction of the South China Sea along the Manila Trench to the

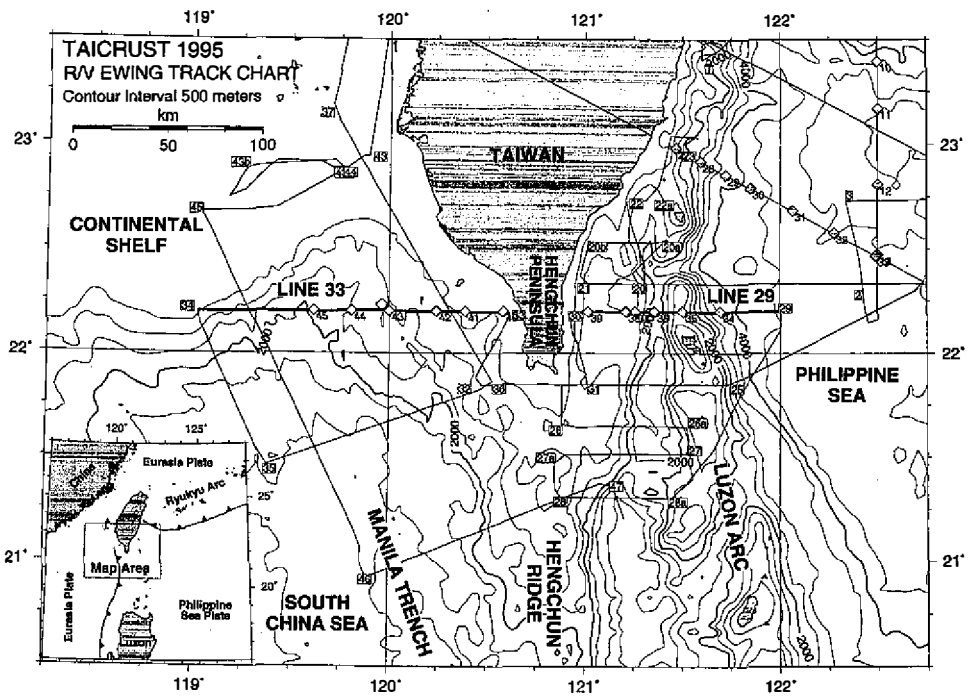

Fig. 1. Seismic lines across Hengchun Peninsula, southern Taiwan. Line 33 lies west of and Line 29 lies east of the peninsula. OBS stations are indicated by diamonds.

south.

The TAICRUST Line 33 west of the peninsula and its companion line, Line 29 to the east of the peninsula, cross this area of incipient collision (Figure 1). Within this area, the Luzon Arc, with its forearc basin and accretionary prism, resulting from the subduction of the South China Sea under the Philippine Sea plate, is beginning to collide with the extended continental crust of the Chinese mainland. The study reported here is an attempt to delineate the deep crustal structure in the area to assist in understanding of the process of the collision.

3. DATA

3.1 Field Experiment

The data reported in this and its companion papers in this volume were acquired using ocean-bottom seismographs (OBSs) of the University of Texas Institute for Geophysics (UTIG) and National Taiwan Ocean University (NTOU). They were the upgraded versions of the digital OBSs described in Nakamura *et al.* (1987) and Nakamura and Garmany (1991). The instruments were deployed along each seismic line from *R/V Ocean Researcher I* ahead of shooting with a large air-gun array of *R/V Maurice Ewing*, and were retrieved after the shooting.

A total of 39 deployments were made along six seismic lines during the experiment, recovering all with full data. The locations of the instruments used in this paper are listed in Table 1. Each UTIG instrument recorded data in four components — gimbal-mounted three-

Table 1. Coordinates of OBS stations on Line 33 and end coordinates of shot lines.[1]

Station	Latitude	Longitude	Depth, m
39[2]	22°11.725'N	121°01.105'E	1232
40	22°11.707'N	120°35.225'E	233
41	22°11.785'N	120°23.557'E	412
42	22°11.860'N	120°14.667'E	831
43	22°11.895'N	120°00.265'E	1144
44	22°11.994'N	119°48.692'E	1533
45	22°12.044'N	119°37.032'E	1812
Line 29 BOL	22°12.039'N	122°00.634'E	
Line 29 EOL	22°11.389'N	120°55.017'E	
Line 33 BOL	22°12.027'N	120°36.082'E	
Line 33 EOL	22°11.381'N	119°00.373'E	

[1]Station coordinates are those recomputed from water-wave arrivals.

[2]Station 39 was on Line 29.

component 4.5-Hz geophones and a hydrophone — while the sole NTOU instrument, at Station 45, recorded data from geophones only. After amplification and anti-alias filtering at 30 Hz (50 Hz for the hydrophone channel), the data were sampled at 4 ms sampling interval and recorded.

3.2 Data Processing and Analysis

The acquired OBS data were first processed through standard processing steps using a software package OBSTOOL (Christeson, 1995). These steps include: (1) computing precise location and orientation of each instrument on the ocean floor using water-wave arrivals (Nakamura *et al.*, 1987), (2) merging with the navigation data, (3) rotating the horizontal axes to radial and tangential directions, and (4) reformatting the data to produce data files in standard SEG-Y format. We used differential GPS (DGPS) navigation data as processed after the cruise by the Institute of Oceanography of National Taiwan University, and applied a correction for the setback of the center of the air-gun array from the GPS antenna to compute the precise location of each shot.

A set of SEG-Y format data tapes thus generated is archived as a permanent record, and used in all subsequent analyses. Generally, the data were further processed through several standard waveform shaping steps such as deconvolution, band-pass filtering and automatic gain control, and were plotted as standard record sections for interpretation. For the analysis reported in this paper, we used a processing package SIOSEIS provided by Paul Henkart of Scripps Institution of Oceanography.

Our analysis of the data to date was mainly to derive a two-dimensional P-wave velocity model of the vertical cross-section below the seismic line. We picked arrival times on the record sections and used forward modeling and inversion to derive a velocity model using the 2-D ray tracing/inversion program of Zelt and Smith (1992). The starting model for this exercise was constructed first by combining the results of layer solutions based on reciprocal arrivals at each pair of stations and arrivals at each station in a split-spread profile configuration, together with the very shallow structures estimated from the coincident multichannel seismic (MCS) record section (Figure 2). Both first and later arrivals were used in this exercise to ascertain inclusion of prominent refractors in the model even when they did not appear as first arrivals.

Although the Zelt and Smith scheme allows one to formally invert arrival times to compute the velocity structure of the model, such inversions as applied to a large region of the model turned out to be unstable because of the complexity of the structure in this area. In particular, large lateral variations, both in geometry of interfaces and velocities within each layer, coupled with relatively large station spacing caused problems. For this reason, the use of the inversion scheme was limited only to certain local regions of the model where such inversion was stable.

As stated above, the analysis is still incomplete. We are currently in the process of applying certain other analysis techniques, including synthetic seismograms and tomographic inversion of first arrival times, but we must defer their results to later papers. Also, the results presented here are based only on vertical geophone data. Analyses of other components,

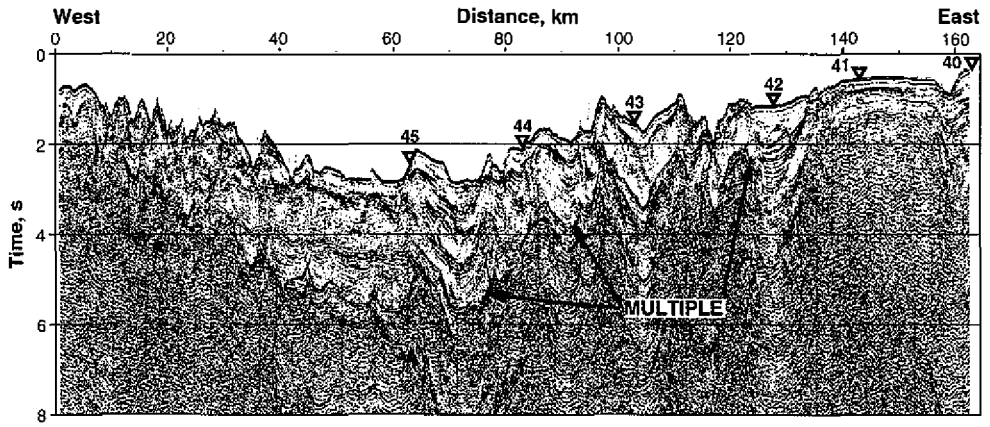

Fig. 2. A multichannel seismic record section showing shallow reflectors under Line 33. OBS locations are indicated by inverted triangles. The vertical exaggeration is 10.7 at sea floor.

especially the horizontal geophone data for converted shear-wave arrivals, are yet to be performed.

4. RESULTS

Figure 3a shows a composite OBS seismic record section displaying record sections of all six OBS stations on Line 33 and the westernmost OBS station on Line 29 aligned in correct spatial relationships. Although some arrivals are not clearly visible at this scale (the original record sections were plotted at a much larger scale), each record section exhibits rather complicated arrivals, reflecting the complexity of the structure under this seismic line.

The first step in interpreting these data is to identify the various arrivals on the record sections. A close examination of the record sections reveals that these arrivals can generally be classified into several groups, as indicated in the accompanied line drawings, Figure 3b. Thus, referring to the figures, the following P-wave arrival groups can be identified based primarily on apparent velocities and offsets: Ps — refracted in the shallow sedimentary layers; Pa — refracted in a margin wedge below the sediments; Pg — refracted in the crustal layers of the subducting slab; PmP — wide-angle reflections from the Moho; Pn — refracted in the upper mantle; and Pl — near-vertical reflections in the sedimentary column.

From the examination of the record sections, it is clear that Pa arrivals are by far the most complex. This suggests that the margin wedge is not a simple uniform prism but large structural variations exist inside. Some arrivals from this layer exhibit large apparent velocity variations within a short distance range, suggesting either reflection or diffraction from irregular interfaces.

Another feature clearly visible on this set of record sections is the trend of the Pg arrivals, arriving later and later from west (Station 45) to east (Station 40). This is a clear indication that the lower crustal layers monotonically dip towards the east under this line.

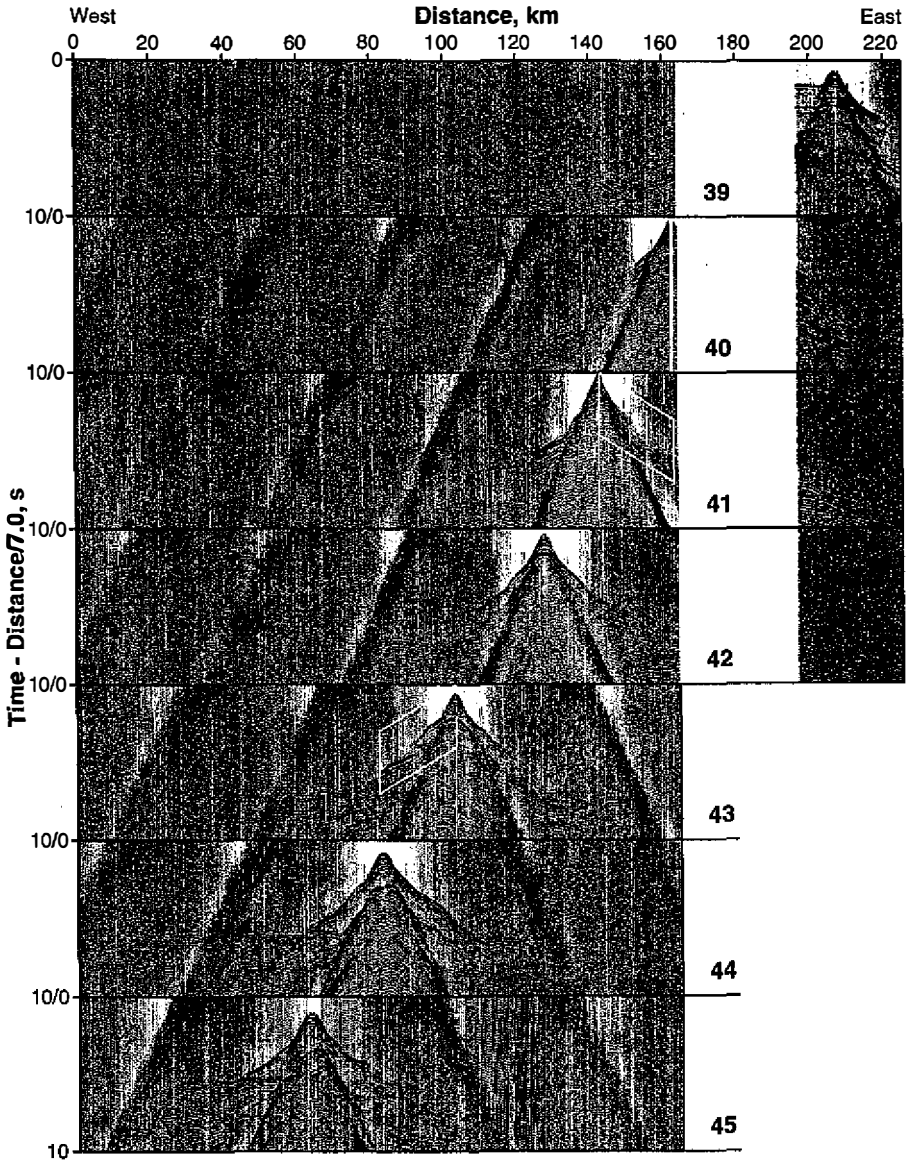

Fig. 3a. A composite OBS record section showing record sections of all six OBS stations on Line 33 and the westernmost OBS station on Line 29 in correct spatial alignment. The horizontal axis is the distance from the west end of Line 33, and the vertical axis is the reduced travel time with a reduction velocity of 7 km/s, covering 0 to 10 seconds downward on each panel. Hengchun Peninsula sits in the gap between 164 km and 197 km in distance. White parallelograms on record sections for stations 41 and 43 indicate the portions shown in Figure 6.

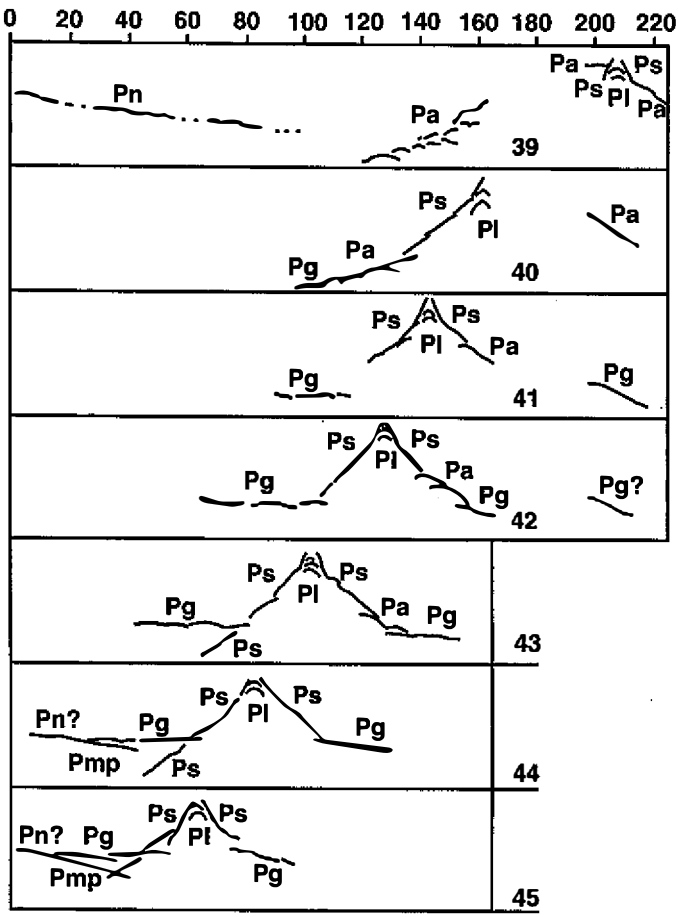

Fig. 3b. A line drawing identifying various groups of arrivals seen on the record section of Figure 3a. See text for identification of labeled arrivals.

Figure 4 shows a P-wave velocity model constructed to fit these arrivals following the procedure described above. As usual, not all model parameters are equally well constrained. As is clear from the ray diagram of Figure 5a, the deep structure at either end of the model is completely unconstrained. Furthermore, the layer thicknesses and velocities are less certain west of station 45 because the model parameters there are based on unreversed seismic arrivals. The same is true with the structure below 6 km depth east of station 40.

Table 2 is a reproduction of summary output from the Zelt and Smith (1992) inversion routine, showing the goodness of fit of arrival picks to the model. The first digit of the phase identification code designates the model layer number and the second digit represents refracted, reflected and head-wave arrivals for 1, 2, and 3, respectively. Note the high χ^2 values for phases 41, 42 and 51. These high values are due to relatively small uncertainty of arrival picks at close distances made on raw (unfiltered) OBS record sections of high quality, which sampled

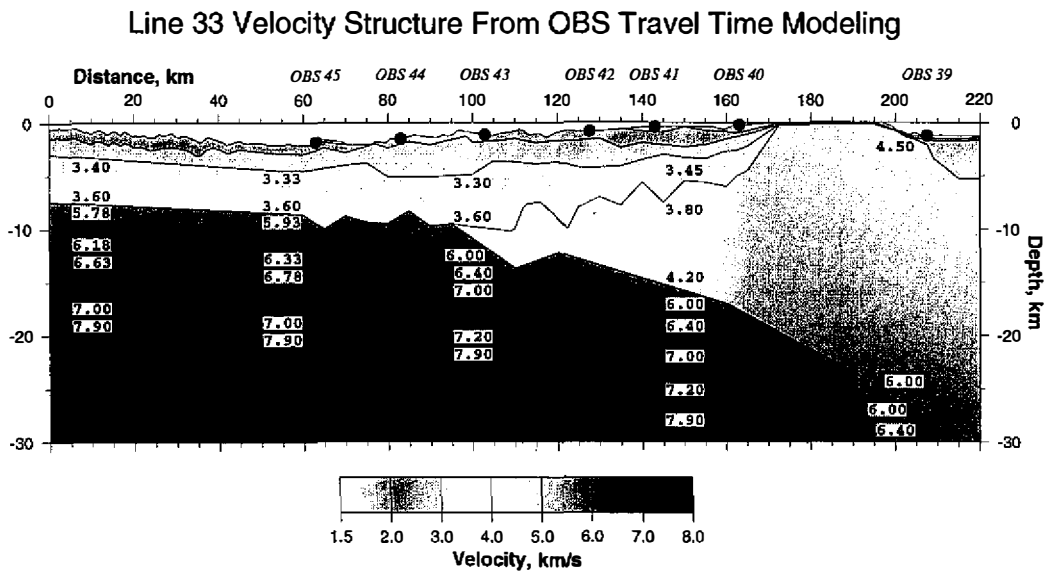

Fig. 4. P-wave velocity model of the structure under Line 33, extending across Hengchun Peninsula to the west end of Line 29. The velocity values shown on the figure are only samples, and larger lateral variations than indicated may exist locally. The velocities in the top three layers generally are: Layer 1 (intermittent) — 1.6-1.9 km/s; Layer 2 — 1.8-2.4 km/s; Layer 3 — 2.5-3.0 km/s. Note that the model parameters west (left) of station 45 are less reliable than others because the non-reversed seismic ray coverage to this area. The vertical exaggeration is 2.5.

structural heterogeneity of smaller scales than the model parameterization intervals. Note also that rms travel time error is within normally acceptable limits for crustal scale modeling. It is quite possible that the velocity variations perpendicular to the seismic line (the 3-D effect) is also contributing to these high χ^2 values. A possible cause of the high χ^2 values for phases 61, 71 and 81 will be discussed later.

In the model, the following main structural components can be identified:

1. The topmost layers of total thickness up to about 8 km in which the P-wave velocity generally increases from about 1.6 km/s just below the sea floor to about 3.6 km/s near the bottom. These layers can be interpreted to be sedimentary layers with the degree of compaction increasing with depth. These layers are thinner near the peninsula.
2. A layer (two layers in the model), about 11 km thick, lying below the sedimentary section with the P-wave velocity generally increasing with depth from about 6 km/s to 7 km/s and dipping gently from west to east. The velocity contrast from the sediment above is distinct. From the seismic velocity and thickness of the layer, it can be interpreted to be extended continental crust which occupied the position between the Chinese mainland and the oceanic basin of the South China Sea. This thickness is within the range of crustal thicknesses

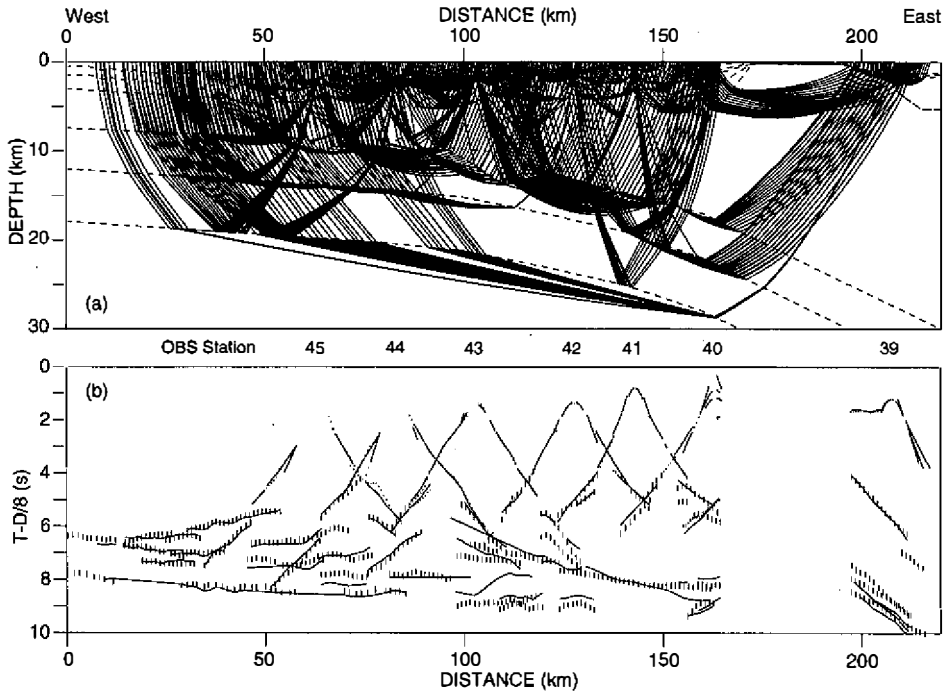

Fig. 5. (a) Ray paths through the model of seismic arrivals used in inversion. (b) Observed (vertical bars) and computed (solid lines) travel times through the model. Only about 15% of the more than 4000 arrivals used in the inversion and their corresponding rays are shown for clarity. The length of each vertical bar expresses the uncertainty of each arrival pick.

in the northern margin of the South China Sea immediately west-southwest of our line as determined by Nissen *et al.* (1995) from two-ship expanding-spread-profile (ESP) data. The dip of this slab appears to increase from about 2° under the western half of the profile to more than 8° as it approaches the peninsula. However, the velocity at the top of the slab becomes indistinct from that of the material above as it dips below the peninsula.

3. A wedge of highly complex structure that lies between the sediments and the slab east of station 43 with average P-wave velocity intermediate to those of the sediments and the slab. This wedge of material has a geometry similar to an accretionary prism associated with subduction of the slab from west to east. Within this wedge, there is a general increase of average velocity from approximately 4 km/s to 5 km/s from west to east. However, the details of velocity variation appear to be far more complex than the velocity variation represented in the model. A comparison of seismic record sections across the wedge shows that arrivals from a series of shots west of the peninsula (Line-33 shots) as observed at a station east of the peninsula are highly irregular with wavy first arrivals, while those from a series of shots east of the peninsula (Line-29 shots) as observed at stations west of the peninsula

Table 2. Statistics of travel-time inversion from xrayinvr routine of Zelt and Smith (1992).

phase	npts	Trms	chi-squared
21	90	0.019	0.908
22	80	0.021	1.168
31	212	0.024	1.453
32	119	0.026	1.712
41	489	0.070	12.304
42	53	0.114	33.260
51	433	0.116	12.582
52	392	0.109	1.184
61	315	0.172	5.274
71	1069	0.368	13.577
81	494	0.240	5.794
82	223	0.164	2.696
83	23	0.180	3.398
91	48	0.115	1.357

are regular with smooth first arrivals (compare arrivals at Stations 39 and 40 in the model distance range of 120-140 km with those at Stations 40 and 41 in the 200-220 km range in Figure 3a). Furthermore, the character of refracted arrivals from this layer (Pa of Figure 3b) is far more complex than those of other arrivals: Numerous closely spaced arrivals follow the first arrival, in contrast to relatively transparent nature of seismic traces following other first arrivals (Figure 6). What is shown in Figure 4 is a result of a relatively simple approach using an irregular interface to model these arrivals. However, despite countless geometrical combinations, all interface patterns we tried resulted in rather high rms errors and large χ^2 values for arrivals 61, 71 and 81 (Table 2), suggesting that another solution may be required. One way to explain this behavior is to introduce some form of alternating high and low velocity layers steeply dipping from west to east inside the wedge, as schematically drawn in Figure 7. To find out the details of this structure requires more closely spaced OBS stations than were used in the experiment, but preliminary synthetic seismograms (work in progress) computed for a structure similar to that of Figure 7 show similar characteristics, reproducing both the contrasting (wavy vs. smooth) shapes of the first arrivals and the enhanced energy following the first arrivals.

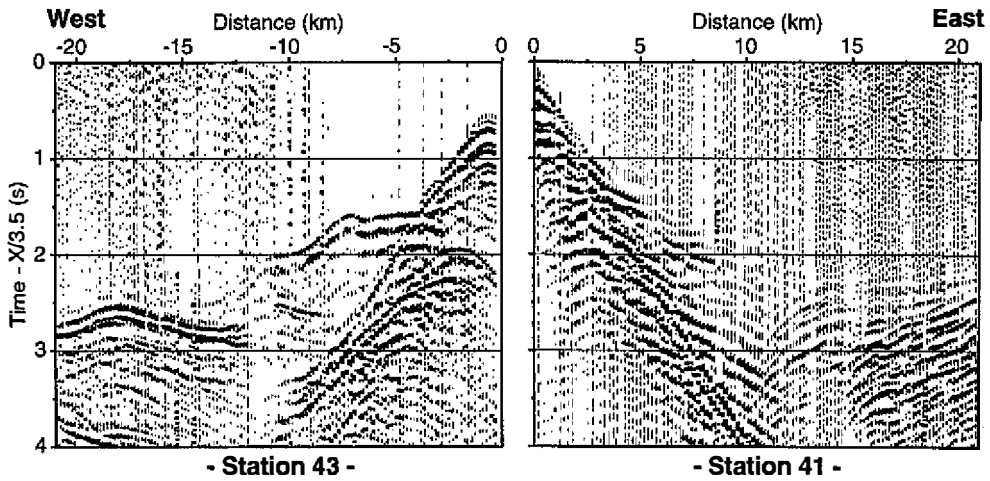

Fig. 6. Sample seismograms showing the complex character of refracted arrivals from the margin wedge (right) compared with more usual arrivals (left). Note the dense arrivals following the rather indistinct first arrivals at distances greater than 11 km at station 41.

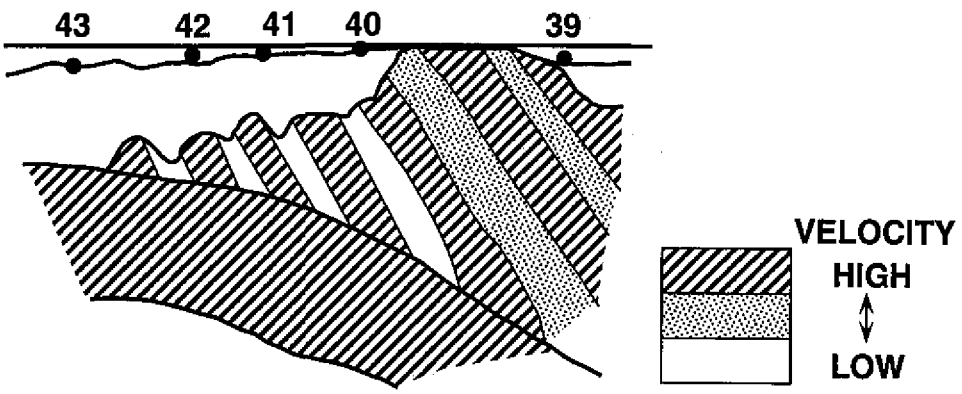

Fig. 7. A schematic sketch of the suggested internal structure of the accretionary prism. The structure is hypothetical, and should not be taken as proven. The actual structure of the accretionary wedge may be much more complex, with gradational changes in seismic velocity.

4. The upper mantle lying at about 18 km depth at the western end of the profile and deepening to greater than 30 km as the line approaches the peninsula. The depth to the Moho and the upper mantle P-wave velocity are relatively well constrained between the model distances of 60 km and 160 km on Figure 4 by the good Pn arrivals observed to distances greater than

200 km from Station 39 (Figs. 3a and 3b) and PmP arrivals observed at several other stations. At the western end of the model, the constraints provided by the unreversed Pn arrivals are such that somewhat deeper Moho, with associated thicker crust, is permissible if accompanied by a faster upper-mantle velocity.

5. DISCUSSION

Although the results reported here are still preliminary, the OBS data have revealed several interesting features under this seismic line. In this section, we will discuss likely geological significance of the main features listed in the preceding section.

The area as a whole is characterized by an extended continental crust of the southern margin of the Chinese mainland subducting under and colliding with the western front of the Philippine Sea plate, which lies east of the study area (see the accompanying paper by Chen and Nakamura in this volume for details of the structure east of Hengchun Peninsula). This collision is a relatively recent phenomenon, or even in its incipient stage, in this part of the plate boundary. As evidenced by the existence of arc-fore-arc-basin morphology to the southeast of the study area, active eastward subduction must be involved in shaping the area, at least in the past if not fully active at present. This process, including earlier subduction of normal oceanic crust, has produced a margin wedge above the subducting slab. As the subducting slab changed its character from pure oceanic to more continental type as the Philippine Sea plate moved northwestward, the subduction may have been impeded somewhat. However, the distribution of earthquake hypocenters and their focal mechanisms (Tsai, 1986; Wu, *et al.*, 1991) suggest that the eastward subduction of the slab under this area is still active, and the present study also shows that the extended continental crust maintains its downward dip toward the east.

Looking at the structure in more detail, the subducting slab is covered with a sedimentary section, about 7 km thick. This compares with the 2-5 km thickness of the syn- and post-rift sediments, mostly from the Chinese mainland, measured along the south China margin to the southwest (Nissen, *et al.*, 1995). The sedimentary section under Line 33 is thicker, which suggests that in addition to the mainland-derived sediments this sedimentary section also includes a significant contribution derived from erosion of rapidly uplifting island of Taiwan as this area lies on the southern edge of the Kaoping slope to the north.

Although the pre-collision structure likely included a sedimentary accretionary prism, the margin wedge built over the subducting slab appears to be more complex than a simple sequence of folds and thrust faults involving the presently observed sedimentary section. The OBS data suggest that the wedge consists of material with an average velocity intermediate to those of the sediments and the slab. Our more detailed, but still tentative, model suggests that eastward dipping layers of alternately high and low velocity may best characterize this wedge. This structural configuration is consistent with development through underplating and/or major out-of-sequence thrusting and which quite likely includes basement complex accreted from the top of the transitional subducting crust.

The material in the wedge was heavily compressed and deformed as it approached the backstop (Luzon Arc), showing relatively high seismic velocity under Hengchun Peninsula

even near the surface. The bottom of the wedge is now seismically indistinguishable from the top of the slab. At its eastern extreme, it becomes of sufficiently high velocity that it is comparable to continental crust in the interpretation of seismic data to the east (Chen and Nakamura, 1998).

Details of the structure under the peninsula, the nature of the backstop and the boundary between the wedge and the advancing front of the Philippine Sea plate are yet to be determined with a combined analysis of the results of this paper together with those from land stations on the peninsula and from other OBSs to the east of the peninsula. However, to find out the detailed internal structure of the wedge may require OBS receiver spacing much closer than that used in the present experiment. The hypothetical structure depicted in Figure 7 should show anisotropy in macroscopic scale, with waves traveling in the lower right-upper left direction, parallel to the layering, exhibiting faster speed than those traveling in the lower left-upper right direction across the layers. In fact, there is a suggestion in the data that this is indeed observed. The arrivals that cross the offshore portion of the wedge, where the ray coverage is more omni-directional than under the peninsula (Figure 5a), tend to be late when the ray crosses the wedge in the lower west-upper east direction and early when the ray crosses the wedge in the upper west-lower east direction (Figure 5b). An experiment may be devised specifically to confirm/refute this observation and thus to test the hypothesis.

6. CONCLUSIONS

A preliminary analysis of the OBS data from a seismic line west of Hengchun Peninsula at the southern tip of Taiwan has revealed that the area is underlain by an 11 km thick extended continental crust subducting at relatively low angle to the east. The thick sediments on top of the subducting slab together with the strong backstop provided by the colliding Philippine Sea plate to the east of the profile are producing a complex margin wedge at depth. The wedge appears to contain high velocity material from deep in the sedimentary section on top of the subducting slab; however, the true nature of the wedge and the backstop is yet to be determined from combined analysis of all the available data.

Acknowledgment We wish to thank the captain and the crew of *R/V Ocean Researcher I*, Cruise No. 429, whose professional assistance made the successful data acquisition possible. Drs. Tan-Kin Wang, Stephane Operto and Chao-Shing Lee, Messrs. Glen Caglarcan, Jack Pitter, Tain-Syh Liu and Miss Julia Liu also participated in the cruise and provided highly valuable assistance. The Station 39 OBS data used in this study were processed by Miss Julia Liu. The DGPS and MCS data were provided to us by Drs. Char-Shine Liu and Philippe Schnürle. The study has been supported by a grant from the National Science Foundation, Grant No. OCE-9417411.

REFERENCES

Chen, A. T., and Y. Nakamura, 1998: Velocity structure beneath eastern offshore of southern Taiwan based on OBS data and its tectonic significance. *TAO*, **9**, 409-424.

Christeson, G., 1995: OBSTOOL: Software for processing UTIG OBS data, Tech. Rept. 134, University of Texas Institute for Geophysics, Austin, 27 pp.

Ho, C. S., 1986: A synthesis of the geologic evolution of Taiwan. *Tectonophysics*, **125**, 1-16.

Huang, C. Y., W. Y. Wu, C. P. Chang, S. Tsao, P. B. Yuan, C. W. Lin, and K. Y. Xia , 1997: Tectonic evolution of accretionary prism in the arc-continent collision terrane of Taiwan. *Tectonophysics*, **281**, 31-51.

Lundberg, N., D. L. Reed, C. S. Liu, and J. Lieske, Jr., 1997: Forearc-basin closure and arc accretion in the submarine suture zone south of Taiwan. *Tectonophysics*, **274**, 5-23.

Nakamura, Y., P. L. Donoho, P. H. Roper, and P. M. McPherson, 1987: Large-offset seismic surveying using ocean-bottom seismographs and air guns: Instrumentation and field technique. *Geophysics*, **52**, 1601-1611.

Nakamura, Y., and J. Garmany, 1991: Development of upgraded ocean-bottom seismograph, Tech. Rept. 111, University of Texas Institute for Geophysics, Austin, 45 pp..

Nissen, S. S., D. E. Hayes, P. Buhl, and J. Diebold, 1995: Deep penetration seismic soundings across the northern margin of the South China Sea. *J. Geophys. Res.*, **199**, 22,407-22,433.

Seno, T., 1977: The instantaneous rotation vector of the Philippine Sea plate relative to the Eurasian plate. *Tectonophysics*, **42**, 209-226.

Tsai, Y. B., 1986: Seismotectonics of Taiwan. *Tectonophysics*, **125**, 17-37.

Wu, F. T., 1991: The modern orogeny of Taiwan. Proc. TAICRUST Workshop, Taipei, 49-62.

Yeh, Y. H., and H. Y. Yen, 1991: Gravity anomalies of Taiwan and their tectonic implications. Proc. TAICRUST Workshop, Taipei, 175-184.

Yu, S. B., D. D. Jackson, G. K. Yu, and C. C. Liu, 1990: Dislocation model for crustal deformation in the Longitudinal Valley area, eastern Taiwan. *Tectonophysics*, **183**, 97-109.

Zelt, C. A., and R. B. Smith, 1992: Seismic travel time inversion for 2-D crustal velocity structure. *Geophys. J. Int.*, **108**, 16-34.